DOI: 10.17725/rensit.2020.12.247

Physical and electrodynamic properties of nanoscale conductive films on polymer substrates

Alim S.-A. Mazinov

Vernadsky Crimean Federal University, https://cfuv.ru/

Simferopol 295007, Russian Federation

E-mail: mazinovas@cfuv.ru

Received March 27, 2020; reviewed April 6, 2020; accepted April 20, 2020

Abstract. **The interaction of high-frequency electromagnetic radiation with thin nanometer-sized aluminum films deposited by magnetron sputtering on flexible polymer substrates has been considered. Experimental studies were carried out on a vector panoramic meter P4226 in the frequency range of 8.2 - 12.2 GHz. The paper reveals the dependences of the relative powers of the reflected, absorbed, and transmitted waves on the film thickness and the relationship between the electrodynamic characteristics and the surface topography.**

Keywords: **microwave radiation, nanoscale films, metal-dielectric structures, absorption coefficient, reflection, transmission, aluminum**

PACS 61.48.+c, 61.66.Hq, 73.61.−r

For citation: Alim S.-A. Mazinov. Physical and electrodynamic properties of nanoscale conductive films on polymer substrates. *RENSIT*, 2020, 12(2):247-252. DOI: 10.17725/rensit.2020.12.247.

Contents

1. INTRODUCTION

The steady increase in the number of mobile radio-electronic equipment: radio stations, smartphones and many other devices [1], together with an increase in intelligence capabilities and a significant reduction in power consumption, results from a decrease in the size of the elements on the integrated circuit (IC), in which conductive tracks and pads make up a significant part [2]. At present, industrial technologies for the production of ICs involve the use of active devices, the sizes of which reach tens or several nanometers [3]. Therefore, the use of conductive films of nanometer thicknesses in the production of electronic components is a future-oriented trend, though further studies of their electrodynamic properties are still needed.

On the other hand, studying the electrodynamic properties of the films are interesting in view of their inclusion in complex metostructures [4], which make it possible to achieve absorption of 80–90% [5]. It should be noted that pure conductive films with thicknesses from 2 to 7 nm can significantly (up to 50%) convert the electromagnetic fields energy of the radio range of 1 ... 400 GHz [6,7] into thermal energy. Although this property of the films limits their use in "conductive" electronics, such resistive properties are useful for stealth technologies [8], as well as for creating thin-film filters, protective shields, or specialized sensors [9].

The topology of the dielectric-metal interface is one of the key issues in creating such absorbing structures as it determines the specifics of the electrodynamic properties of the structure as a whole [10]. Most of the research work on this topic deals with the

study of the interaction of radiation and metal-dielectric structures based on solid substrates [11, 12]. However, the prospects for creating flexible devices, as well as the possibility of simplifying the production of flexible screens and antennas, require special consideration of the interaction of electromagnetic radiation with a metal-dielectric structure on polymer substrates [13]. Consequently, the aim of the present paper is to identify the specifics of the interaction between electromagnetic radiation from the microwave range and the MDS, in relation to the surface geometry of the flexible substrate.

2. THE EXPERIMENTAL RESEARCH TECHNIQUE AND THE OBJECT OF THE RESEARCH

Studies of the relative powers of reflected, transmitted, and absorbed waves (optical coefficients) in the range 8.2–12.2 GHz were carried out using the Mikran P4226 vector network analyzer (**Fig. 1**). To obtain normalized data and calculate the losses of the waveguide system, at the beginning and end of the experiment, the measurements of the parameters on clean flexible substrates were made with an attached 200 μm thick aluminum plate, exceeding the skin layer for the conductor at the lower boundary of the working frequency range. To compensate for the influence of coaxial-waveguide transitions, as well as other factors, calibration was performed using a reflection measure and a quarter-wave line (TRL: Thru, Reflect, Line) [14], which made it possible to obtain fairly accurate results.

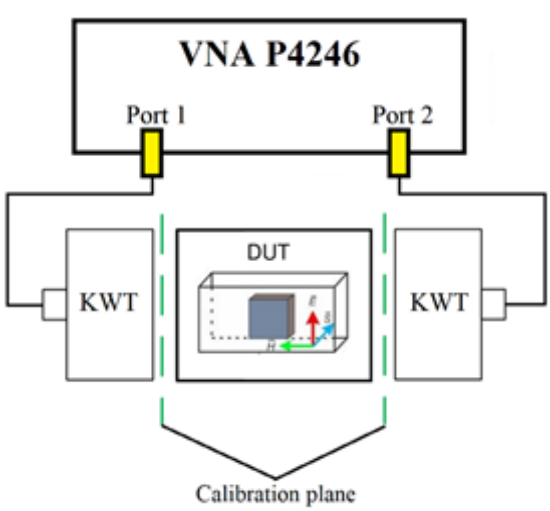

Fig. 1. *Installation block diagram.*

The direct interaction between the microwave and the samples was determined by the matrix of S-parameters, the main components – S21 and S11 – corresponding to a direct drop from the first port, were chosen. As the initial measurements showed, the properties of the measuring waveguide path, with the structure under study, are close to the properties of a reversible four-terminal circuit, i.e. the transmission coefficient is the same in both directions. Accordingly, we used the main components S21 and S11, corresponding to a direct drop from the first port of the vector analyzer. The coefficients of transmitted, reflected and absorbed power were determined using the obtained S-parameters (Fig. 2):

$$T = \frac{P_{thru}}{P_{inc}} = \frac{|V_{thru}|^2}{|V_{inc}|^2} = |S_{21}|^2,$$

$$R = \frac{P_{reflect}}{P_{inc}} = \frac{|V_{reflect}|^2}{|V_{inc}|^2} = |S_{11}|^2,$$

$$A = 1 - |S_{11}|^2 - |S_{21}|^2.$$

Metal-dielectric structures were fixed in the geometric center of the waveguide path, perpendicular to the axis of the waveguide with standard dimensions of 23×10 mm. To avoid the capacitive and inductive effect of metallization on the measuring system, the effective area of interaction of radiation and the samples was 10% of the waveguide area - 6×6 mm. The samples were placed on the geometric center of the waveguide cross section and were fixed by a dielectric substrate made of synthetic foam, "transparent" for electromagnetic radiation. Thus, the sample was affected by the maximum power of H10

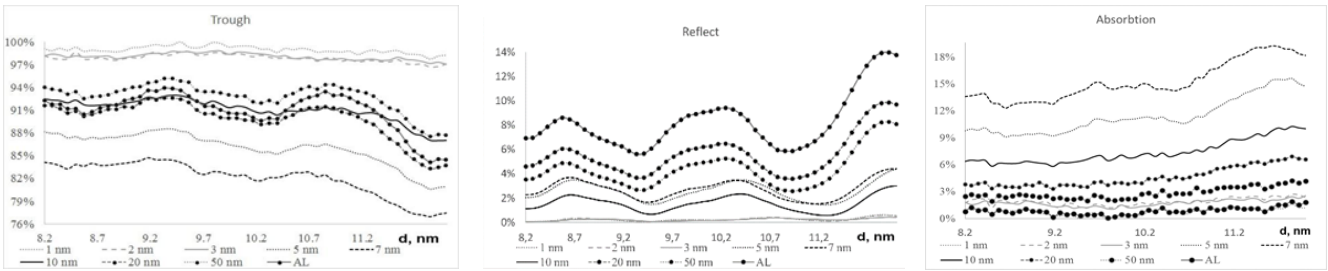

a b c

Fig. 2. *Frequency dependences of the coefficients: a - passage; b - reflection; c - absorption.*

wave electric field and the major part of the wave energy interacted with a nanoscale conducting film.

Films made of lavsan (polyethylene terephthalate), fluoroplastic and teflon were taken as the basis for MDS. This paper presents the results of studying MDS with lavsan films, since the results involving the study of fluoroplastic and teflon substrates differ insignificantly. The conductive part was deposited by the method of magnetron sputtering of the target using the URM 3.1279.0129 installation with additional ion beam processing. What is more, the planetary rotation of the substrates ensured uniform coating deposition, and in combination with adjusting the deposition time, it was made possible to obtain a range of the conducting layers thicknesses: 1, 3, 5, 7, 10, 20, 50 nm.

The initial assessment of the substrates surfaces of was carried out using an optical interference microscope LOMO MII-4M in broadband radiation of a white LED with subsequent detailing of the relief using red and blue lasers. A more detailed analysis of the formation process and morphological characteristics of aluminum nanofilms was carried out using an NT-MDT nanoeducator 2 scanning atomic force microscope, to compare them with the absorption, transmission, and reflection spectra.

3. DISCUSSION OF THE RESULTS

Along with a number of advantages, there is one more benefit to the method of using 10% of the interaction area in the waveguide – its significant sensitivity to diffraction. As a result, a monotonic decrease in the transmission coefficient T (Fig. 2*a*) and an increase in the reflection coefficient R (Fig. 2*b*) for thin conducting films do not correlate with theoretical calculations, which show independence of T, R on the frequency and, accordingly, independence of the absorption A on the frequency as well [6,15]. This is not due to the specifics of the physical properties of active MDS, but is accounted for by a decrease in the diffraction properties of the object under study with a decrease in the wavelength.

In accordance with the established concepts, the reflection coefficient should vary from the minimum value corresponding to the substrate without metal ($d = 0$), and monotonically increase to the value corresponding to the formed film ($d > 15 \ldots 20$ nm). However, in the range of film thicknesses $5 < d < 10$ nm, there is a deviation from the monotonicity of the reflection coefficient growth (Fig. 2*b*), which is associated with the relief of the film.

The maximum absorption of an aluminum film on lavsan is achieved at the conducting layer thickness $d = 7$ nm (Fig. 2*c*). This is due to the transition of the MDS from the dielectric ($d = 0$) with the geometric dimensions of 6×6 mm, to film structures of greater thickness, causing electric short circuiting of the space. This leads to a change in conductivity from 0 to values characteristic of the bulk of a continuous material, in our case Al $\sim 3.8 \cdot 10^7$ S/m. It is with the thickness $d = 7$ nm that the specific conductivity reaches about 10^6 S/m [6,

9], and there occurs the maximum conversion of the induced currents to thermal energy.

For an in-depth understanding of the nature of the nonlinear interaction effect at the thickness of 7 nm, the growth dynamics of a conductive material on a flexible substrate was analyzed.

4. THE CORRELATION BETWEEN ELECTRODYNAMIC CHARACTERISTICS AND FILM MORPHOLOGY

A general analysis of surface morphology, carried out by a sequential study of optical microscopy with subsequent analysis of AFM images, revealed a more complex surface morphology of MDS on flexible substrates compared to solid ones [16]. From an aggregate analysis of profilograms, it follows that the polymeric substrate made of lavsan has relatively large height differences (**Fig. 3***a*), however, in contrast with solid amorphous substrates, the change in height occurs rather slowly and smoothly, within small areas, and the surface is quite smooth (PTFE and Teflon films have similar the reliefs). It should be noted that the surface of the substrate was not pre-processed.

After deposition of aluminum with the thickness of 5 nm (Fig. 3*b*), lateral micro-formations, reaching tens of nanometers in height, are visible on the substrate. With longer spraying, the number of conductive micro-formations increases significantly (Fig. 3*c,d*). With an approximate coating thickness of 10 nm (Fig. 3*d*), the formation of a smoother surface in observed in the AFM image, with elevation drops larger than 7 nm.

The quantitative analysis of the correlation between the electrodynamic parameters of the radiation effects and the surface topology was based on statistical data and the root-meansquare value of roughness (*Zq*), which was determined by measuring the value of the deviations from the midline:

$$Zq = \left(\frac{1}{N} \sum_{j=1}^{N} z_j^2 \right)^{1/2},$$

where z_j is the deviation of the j-th point, N is the number of points in the image.

A non-standard increase in the absorption coefficient for films with thicknesses of 7 nanometers correlates quite well with the dependence of *Zq* on their thickness (**Fig. 4**). A sharp increase in the root-meansquare

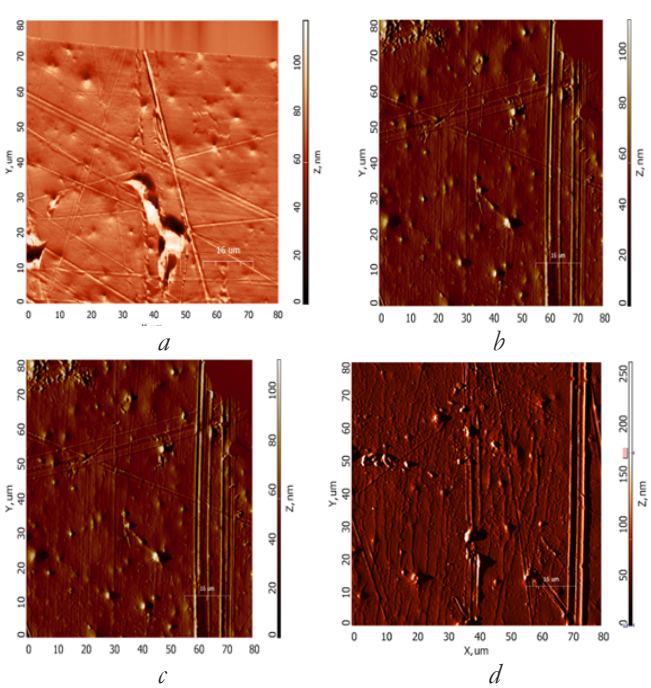

Fig. 3. *Dynamics of changes in the surface morphology using a border detection filter (Pruitt filter): a - clean substrate; b - 5 nm aluminum film; c - thickness 7 nm; d - thickness of 10 nm.*

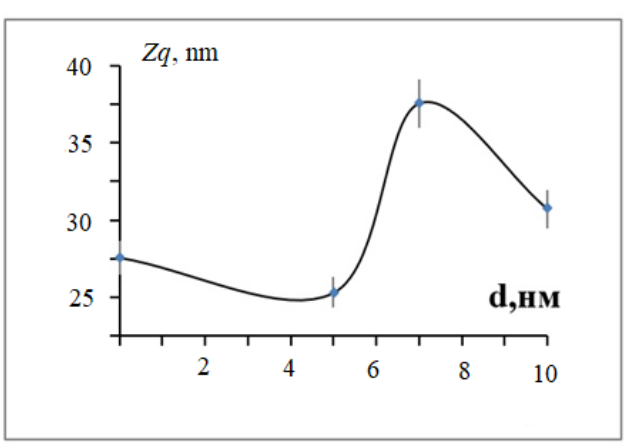

Fig. 4. *The dependence of the change in the root mean square roughness on the thickness of the coating.*

value of roughness of the coating indicates a transient process of the conversion of localized nano and micro objects into a continuous conductive layer, which leads to an increase in the total conductivity. An intermediate step in this process is the formation of "bridges" between metal formations, which is the reason for the growth of *Zq*. However, the average conductivity of the floor bridges at the initial stage of growth is small, as is the conductivity of the crystallites themselves at small sizes, taking into account possible oxidative processes. Therefore, part of the induced incident microwave energy of alternating current is transformed into Joule heat on a non-ideal conductor.

The increase in the reflected wave energy at thicknesses of more than 10 nm (Fig. 2*b*) is accounted for by the increase in induced currents, which include inductive and capacitive components. The general conduction currents, in turn, are due to the emergence of stable galvanic bonds between individual conductive islands and the primary growth of connecting "bridges", as confirmed by a sharp decrease in *Zq* at an increase in the conductive layer thickness (Fig. 4). A further process of the conductive material deposition leads to the formation of a continuous conductive film having not only a uniform atomic structure, but also sufficient uniformity in thickness, which is exactly due to the relatively smooth surface of the substrate. This, in turn, leads to a sharp increase in conductivity, approaching the conductivity of a bulk material, which leads to an increase in the conversion of the incident wave into the reflected wave by means of increased currents.

5. CONCLUSION

The study of the interaction of EMR and MDS on flexible substrates showed the identical nature of absorption, as well as it did in their solid-state counterparts, the main feature being the absorption coefficient peak occurring within a small range of the conductive layer thickness. A feature of the interaction of electromagnetic radiation and a flexible layered structure of aluminum-lavsan is the resonance at the thickness of 7 nm, which is greater than that of similar solid structures.

In the case of our study, the key point determining the reflection and absorption of MDS was the modification of the resistive properties of the aluminum conductive layer. It is the specifics of the lavsan surface geometry, where smoother peaks were observed between the heights of 100-150 nm, that formed the conductive layer by means of islands, which were connected by bridges as they increased. Exactly at the instance of the conductive bridges formation in the structure, the conductivity arises, converting the energy of the incident radiation into joule heat. Further growth of the conductive layer leads to smoothing of the relief and forming a continuous structure with conductivity approaching that of the bulk, thereby increasing the reflected wave fraction.

REFERENCES

1. Konstantinou D, Bressner TAH, Rommel S, Johannsen U, Johansson MN, Ivashina MV, Smolders AB, Monroy IT. 5G RAN architecture based on analog radio-over-fiber fronthaul over UDWDM-PON and phased array fed reflector antennas. *Optics Communications,* 2020, 454:124464, doi: 10.1016/j.optcom.2019.124464.
2. Hills G, Lau C, Wright A. Modern microprocessor built from complementary carbon nanotube transistors. *Nature,* 2019, 572:595-602, doi: 10.1038/s41586-019-1493-8.
3. Khan HN, Hounshell DA, Fuchs ERH. Science and research policy at the end of Moore's law. *Nature Electronics,* 2018, 1(2):146–146, doi: 10.1038/s41928-017-0005-9.

4. Yuan J, Liu Q, Li S, Lu Y, Jin S, Li K. Metal organic framework (MOF)-derived carbonaceous Co 3 O 4 /Co microframes anchored on RGO with enhanced electromagnetic wave absorption performances. *Synthetic Metals,* 2017, 228:32-40, doi: 10.1016/j.synthmet.2017.03.020.
5. Tran MC, Pham VH, Ho TH, Nguyen TT, Do HT. Broadband microwave coding metamaterial absorbers. *Scientific Reports,* 2020, 10(1):1810, doi: 10.1038/s41598-020-58774-1.
6. Nimtz G, Panten U. Broad band electromagnetic wave absorbers designed with nano-metal films. Ann. Phys. (Berlin), 2010, 19(1-2): 53-59. DOI 10.1002/andp.200910389
7. Li S, Anwar S, Lu W, Hang ZH, Hou B, Shen M, Wang CH. Microwave absorptions of ultrathin conductive films and designs of frequency-independent ultrathin absorbers. *AIP Advances*, 2014, 4(1):017130, doi: 10.1063/1.4863921.
8. Ahmad H, Tariq A, Shehzad A, Faheem MS, Shafiq M, Rashid IA. Stealth technology: Methods and composite materials-A review. *Polymer Composites,* 2019, 1:16. DOI: 10.1002/pc.25311.
9. Vdovin VA. Nanometer metal films in the sensors of powerful microwave pulses. *III All-Russian Conference "Radar and Radio Communication". IRE RAS*, 2009, 832-835.
10. Fitaev IS, Orlenson VB, Romanets YV, Mazinov AS. Surface topologies of thin aluminum films and absorbing properties of metal dielectric structures in the microwave range. *ITM Web of Conferences,* 2019, 30:08013, doi: 10.1051/itmconf/20193008013.
11. Andreev VG, Vdovin VA, Pronin SM, Khorin IA. Measurement of optical coefficients of nanometer metal films at a frequency 10 GHz. *Journal of Radio Electronics (IRE RAS),* 2017, 11:4.
12. Zuev SA, et al. Microwave Range Diffraction Properties of Structures with Nanometer Conductive Films on Amorphous Dielectric Substrates. *26th Telecommunications Forum (TELFOR*), 2018, 1-4, doi: 10.1109/TELFOR.2018.8611867.
13. Antonets IV, Kotov LN, Makarov PA, Golubev EA. Nanostructure, conductive and reflective properties of thin films of iron and $(Fe)_X(BaF_2)_Y$. *Journal of Technical Physics*, 2010, 80(9):134-140.
14. Guba VG, Ladur AA, Savin AA. Classification and analysis of calibration methods for vector network analyzers. *TUSUR Reports*, 2011, 2(24):149-155.
15. Orlenson VB, Zuev SA, Starostenko VV. *ITM Web of Conferences CriMiCo'2019,* 2019, 30:08011, doi: 10.1051/itmconf /201930 ITM.
16. Starostenko VV, Mazinov AS, Fitaev IS, Taran EV, Orlenson WB. The dynamics of the surface formation of conductive aluminum films on amorphous substrates. *Applied Physics*, 2019, 4:60-65.